ChemComm

Accepted Manuscript

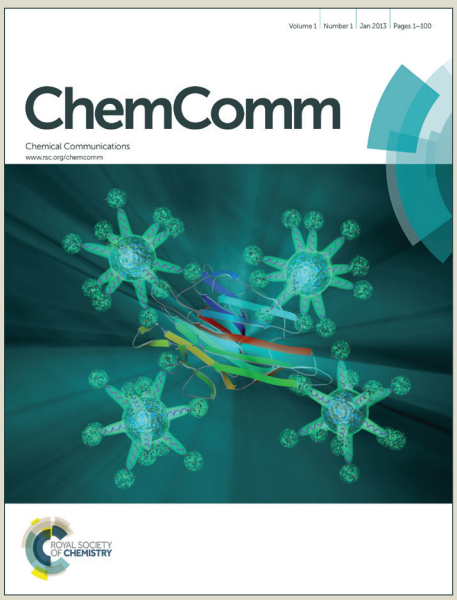

ROYAL SOCIETY OF CHEMISTRY

www.rsc.org/chemcomm

ChemComm

RSCPublishing

FEATURE ARTICLE

Using Cell Structures to Develop Functional Nanomaterials and Nanostructures – Case Studies of Actin Filaments and Microtubules

Cite this: DOI: 10.1039/x0xx00000x

Received 00th January 2012,
Accepted 00th January 2012

DOI: 10.1039/x0xx00000x

www.rsc.org/

Kevin Chia-Wen Wu,†[a] Chung-Yao Yang†[b] and Chao-Min Cheng*[b]

This article is based on the continued development of biologically relevant elements (i.e., actin filaments and microtubules in living cells) as building blocks to create functional nanomaterials and nanostructures that can then be used to manufacture nature-inspired small-scale devices or systems. Here, we summarize current progress in the field and focus specifically on processes characterized by 1) robustness and ease of use, 2) inexpensiveness, and 3) potential expandability to mass production. This article, we believe, would provide scientists and engineers a more comprehensive understanding of how to mine biological materials and natural design features to construct functional materials and devices.

Introduction

Humankind often derives guidance and inspiration from nature, a wellspring for elegant, complex, integrated, and optimized structural solutions that enable organisms to accomplish complex functions. Unfortunately, many scientists approach design without any explicit reference to nature, as direct natural analogs do not exist for many associated technological applications. In recent years however, there has been increasing interest in borrowing design concepts or materials from nature to create small-scale functional materials, structures, and systems. Nanomaterials such as inorganic nanowires, metal-based nanowires or nanoparticles (NPs), quantum dots (QDs), or carbon nanotubes demonstrate promising optical, electronic, and catalytic properties. Biomolecules, such as DNA, enzymes, or antibodies contain dimensional similarities with these nanomaterials and suggest that the combination/integration of biomolecules with nanomaterials may develop hybrid systems that leverage collective properties.[1] Considerable previous accomplishments, over recent decades, has advanced the development of biomolecule-conjugated nanomaterials or nanostructures and their applications for nanoscale machinery, sensing, logic operations, and nanodevices.[1] However, little of this work has been directed toward developing a system in which both bio- and nano-sourced building block contributors have mutually benefited and, in paired combination, improved final functional properties of the "marriage" using either microtubules or actin filaments.

The design of functional organic nanostructures using biotemplating is still an almost unexplored field. In this article, we attempted to summarize current progress in the field and focus specifically on processes characterized by 1) robustness and ease of use, 2) inexpensiveness, and 3) potential expandability to mass production, through the novel use of actin filaments and microtubules.

The cytoskeleton is a filamentous network of F-actin, microtubules, and intermediate filaments composed of one of the three chemically distinct subunits, actin, tubulin, or one of several groups of intermediate filament proteins. The complex dynamics of actin filaments and other cytoskeletal elements play an important role in multiple cellular behaviors such as cell division, motility, and determination of cell shape.[2] Cytoskeletal filamentous (F-) actin, a double-stranded helical filament made of globular actin (G-actin), is, essentially, a semiflexible polymer and highly charged polyelectrolyte, with a diameter of ~8 nm and a persistence length of ~10 μm.[3] Examination via X-ray diffraction and small-angle X-ray scattering could indicate the presence of minute structural elements such as filaments, bundles, and networks at the molecular level that could provide insight into the interactive process of self-assembly of biological polyelectrolytes like actin.[4]

Actin, an intracellular structural protein, plays a crucial role in a wide range of cellular behaviors, including the migration of eukaryotic cells, their mitosis, and their shape (mechanical integrity).[5] Actin stress fibers, have also been known to actively remodel in response to cyclic strains, as demonstrated in cultured bovine aortic endothelial cells.[6] In the cyclic strain research that demonstrated this remodelling, bovine aortic endothelial cells were seeded on fibronectin-coated silicone membranes and subjected to either uniaxial or biaxial

sinusoidal stretching at a controlled frequency. Both of these dynamic loading conditions caused an increase in actin stress fiber density, but the changes in fiber orientation were distinct, as the output responses in these two techniques diverged. Frequency imposed *uniaxial* stretching induced stress fibers to orient themselves perpendicular to the axis of stretching, while *biaxial* stretching did not result in any specific fiber orientation.[7] Such alignment of stress fibers in the direction of the minimal substrate deformation has also been reported by Wang *et al.*[8]

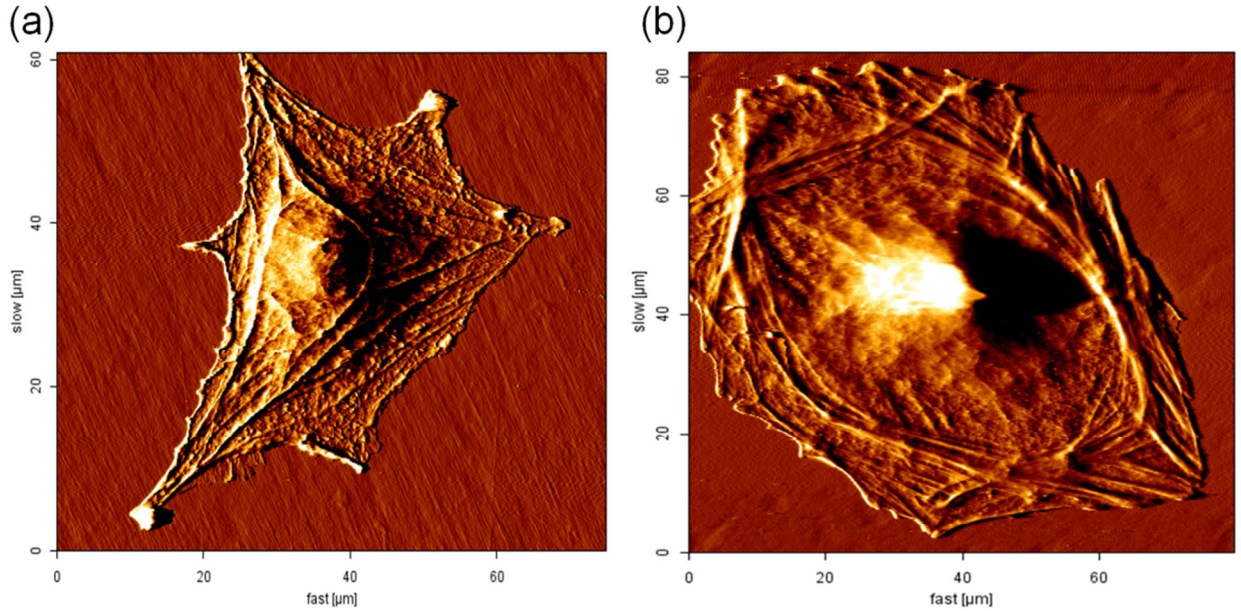

Fig. 1 (a) Revealing actin filaments from a living 3T3 fibroblast using an AFM. A living 3T3 fibroblast was seeded on a glass coverslip coated with type I collagen, and mounted onto a Bio-Cell (JPK Instrument, Germany) temperature-controlled sample holder filled with DMEM containing 10% FBS as culture media. A Nano Wizard II (JPK Instruments, Germany) AFM was used to scan the cell in liquid under contact mode. Silicon nitride cantilevers (CSC-38B, MikroMasch) with a nominal spring constant of 0.03 N/m [calibrated using the thermal noise method] and cone half angle <15° were used for imaging. Prior to scanning, the scanning range of the AFM cantilever tip was positioned to ensure full coverage of the cell. The cell was then scanned with tip velocity controlled between 90-110 µm/sec and force applied between 0.5~1.0 nN. The whole scanning time was kept under 15 minutes to minimize the changes in cytoskeleton throughout the process. The image file was processed using JPK data analysis software (JPK Instruments, Germany), where the deflection, height, three-dimensional, and cross section profile images could be extracted. The location of the actin filaments was previously identified by comparing the scanned image of actin-RFP-3T3 cell and its respective fluorescent image, where prominent actin filaments could be observed. The linear filamentous structures were shown to be actin filaments. (b) Revealing the cortical actin filaments of a living PK-1 (Porcine Kidney-1) epithelial cell using an AFM. Notice the actin filaments in this cell are shorter comparing to those of the fibroblasts, and located mainly on the cell periphery, fitting the description of so-called "cortical actin." (a) & (b) were experimental work contributed by Hans Harn and Dr. Yao-Hsien Wang of Dr. Ming-Jer Tang's lab, respectively.

Fig. 1 reveals the actin filaments of a living 3T3 fibroblast and porcine kidney-1 epithelial cell via liquid-type atomic force microscopy. It is well documented that mammalian cells subjected to cyclic mechanical strain transmit this mechanical force into intracellular signals and induce cellular responses, and may suppress apoptosis.[9] These results indicate that cell proliferation would be enhanced by cyclic mechanical stimulation. Physiomechanical stress affects the cytoskeleton and plays an important role in determining and maintaining cellular function. As with the physiomechanical stress or stimulation, thermal change/stimulation is likely to impart significant conformational changes to actin via the cytoskeleton. This is based on our own previous research in which we investigated cytoskeletal conformation changes in NIH-3T3 fibroblasts after a single heat shock treatment (37°C to 43°C).[10] In this work, with respect to cytoskeletal organization, we have found that the cytoskeleton approached original polymerized organization following heat shock, but did not completely return to the original state. At high temperatures, the lipid bilayer of cell membranes can dissociate. Resulting changes in membrane potentials could induce many possible changes in cellular function resulting from the loss of proteins critical for maintaining bilayer integrity.[11]

Microtubules (MTs) are cytoskeletal, self-assembling, dynamic, tubular structures with nanometerically sized diameters and an average length of 25 µm.[12] The cross-section of a MT will show a ring with inner and outer diameters of approximately 16 and 24 nm, respectively. Microtubules have several functions, e.g., they form the cytoskeleton lattice in the cytoplasm of eukaryotic cells. As tracks for transporting particles in the axonal MTs, MTs generate forces for movement in flagella and cilia. They also play an essential role in mitosis during cell division. Microtubule formation can be mimicked *in vitro* through the addition of guanosine-5'-triphosphate (GTP) to a solution of the α- and β-tubulin heterodimer.[13] Clearly, combining biomolecules with nanomaterials represents an area of considerable promise and an intriguing array of possibilities in the area of materials science. As a result of great interest and novel research, MTs have been used to initiate transport of biomolecules on engineered surfaces and to study the

biochemistry of motor proteins.[14] In this article, we wish to accomplish two objectives: 1) outline current progress; and, 2) suggest ways to overcome any obstacles inherent in making functional nanomaterials, nanostructures, and (ultimately) nanosystems using biologically relevant elements, i.e., actin filaments and MTs in this article. Our goals are based on research and significant interest generated in multiple academic communities including nanomaterials (materials, chemical science), nanotechnology (engineering, applied physics) and biotechnology (cell biology, bioengineering).

Preparation of individual actin filaments and microtubules *in vitro*

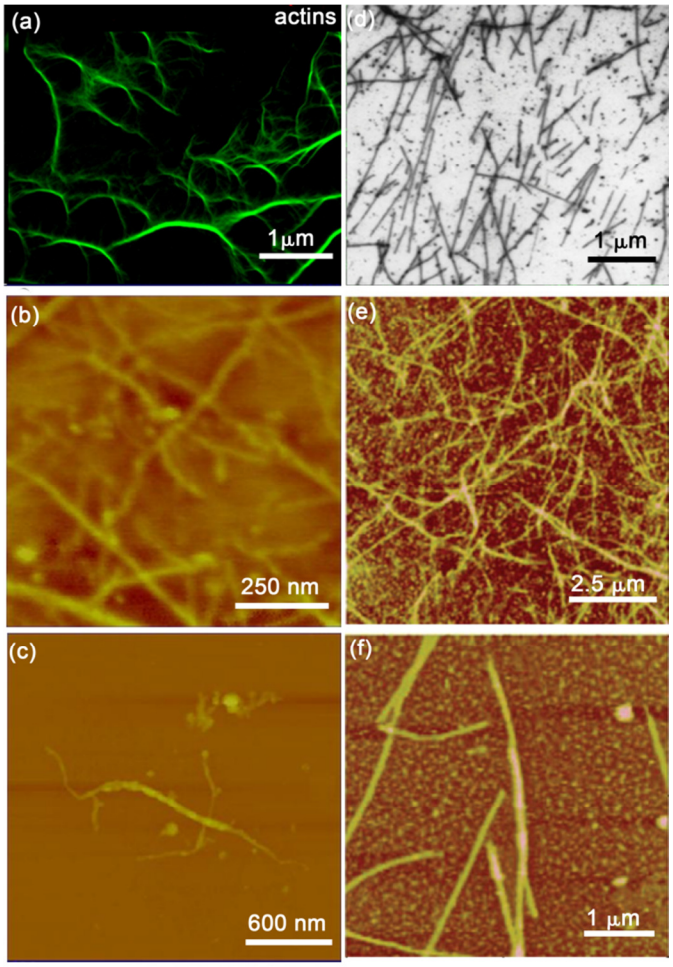

Fig. 2 Fluorescence images of (a) F-actin. F-actins were stained with 6 μM Alexa Fluor 488 phalloidin. The samples were examined under an epi-fluorescent microscope (Zeiss Axiovert, Germany) equipped with a 63X high numerical aperture (NA = 1.4) oil immersion objective to image the actin filaments (Scale bar = 1 μm). In (a), the image shows that actin filaments have condensed into a parallel arrangement and have an ensemble of thick bundles. It is noted that dramatically increased fluorescence intensity from the multifilament bundles. (b) and (c) are atomic force microscopy images of the actin filaments; (b) morphology of a single actin filament with a length of 100 nm and (c) the matrix of the actin filaments. (d) SEM image of brain microtubules assembled after a single polymerization cycle. (e) AFM topography images of polymerized microtubules adsorbed to silanized mica where a few individual microtubules with a well preserved structure are easily observed. (f) A microtubule-rich region in the sample showing contaminant material; (d-f) are from Ref. 18d.

For the preparation of individual actin cytoskeleton *in-vitro*, we describe one of the commonly used procedures.[15] F-actin in an ATP-buffer[16] or phosphate buffered saline solution (PBS, from *Fisher*) was first prepared. The steps to perform this were as follows: (1) 1 mL of ATP-buffer was combined with 2 μL pure ATP (100 mM); (2) G-actin was re-suspended to obtain a concentration of 0.4 mg/mL; (3) this solution was mixed and incubated for one hour at 24°C after adding 66 μL ATP polymerization buffer (from *Cytoskeleton, USA*; No.: BSA02);[17] and, (4) 2 mL Milli-Q water was added to the solution, which was then kept in liquid nitrogen (-70°C) for one hour with the diluted G-actin before incubating for one hour at 24°C. Fig. 2a contains images of the polymerized actins that were 5~10 μm length; these were created with different concentrations and labeled with phalloidin (from *Molecular Probes, USA*; No.: A12379). The samples were examined under a fluorescent microscope (Zeiss Axiovert, Germany) using a 63X high numerical aperture (NA = 1.4) oil immersion objective to image the G-actin monomer aggregates and F-actin. We also imaged the filamentous actin using an atomic force microscope (AFM) in an aqueous environment as shown in Fig. 2b. This displays not only the distribution of actin filaments in a network, but also a higher resolution portrayal of individual actin filaments on the surface of the material. We continued to probe the behaviour of F-actin by obtaining the deflection-displacement curve via AFM for single actin filaments with a silicon nitride tip (spring constant of a cantilever is 0.2 N/m); the adhesive force of the silicon nitride tip on the single actin filament was between 0.15 and 2 nN (Fig. 2c).

For the preparation of individual MTs *in vitro*, many similar MT protein purification methods have been developed.[18] In this study, we describe one of the commonly used procedures. Tubulin was purified from porcine brains by two assembly disassembly cycles and phosphocellulose chromatography, and stored in liquid nitrogen at 6 mg/mL. Tubulin was polymerized into MTs in BRB80 buffer (1 mM EGTA, 1 mM $MgCl_2$, 80 mM PIPES–NaOH) containing 1 mM GTP and 1 mM $MgSO_4$. After incubating at 37°C for 30 minutes, MTs were stabilized and diluted 100X in BRB80 containing 20 mM toxal.[18d] Fig. 2d displays SEM images of the polymerized MTs that were 500 nm ~ 1.5 μm length; these were assembled after a single polymerization cycle. Fig. 2e and 2f show AFM images of MTs adsorbed to mica functionalized with APTES, a silane with an amine group that is positively charged at ~ pH 7. Since mica is composed of multi-layers, which can be peeled to generate a new clean surface without any preliminary washing procedures (unlike traditional glass). Microtubules on mica were observed in tapping mode at atmosphere in order to minimize de-adsorption. Fig. 2e displays a microtubule-rich region in the sample showing contaminant material. AFM topography images of polymerized MTs adsorbed to silanized mica where a few individual MTs with a well preserved structure are easily observed (Fig. 2f).

Various applications of using actin/microtubule cytoskeleton *in vitro*

Actin has long been known for providing strong structural support for cells and for acting as a linker for protein motor systems important in biological systems. To date, several studies have reviewed the structure, mechanism, and mechanical strength of self-assembling actin and actin's interactions with other biomolecules.[19] Beyond examination of these more fundamental studies, there is growing interest and research into the use of actin/MTs for a range of applications (Fig. 3) because actin exhibits several advantages: 1) excellent biocompatibility: 2) robustness and ease of use: 3) inexpensiveness: 4) realizable and precise control of self-assembled structure: and, 5) potential expandability to mass production. Herein, several potential applications of actin/MTs including drug delivery, patterning, and nanofabrication are introduced.

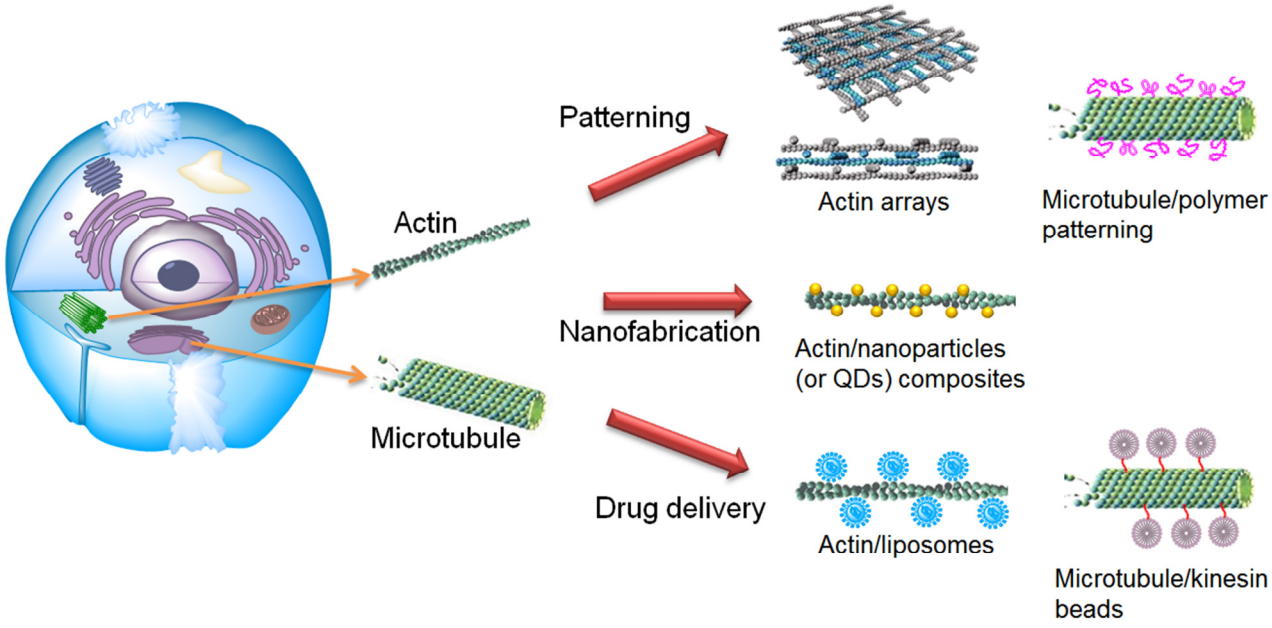

Fig. 3 Schematic demonstrating the production of functional materials, structures, and systems at the nanometer scale using actin and microtubule cytoskeleton.

Drug delivery

Actin, the major component of the cytoskeleton, provides functional mechanical stiffness for cells. Inspired by its role in cellular architecture, several research groups have used actin filaments to stabilize the structure of liposome-based drug nanocarriers because plain liposomes generally decompose when they are exposed to fluid shear stresses.[20] Cortese *et al.* compressed actin filaments inside the core of liposomes and found that the deformation of liposome was dependent on the length of encapsulated actin filament.[20a] Miyata and Hotani found that G-actin-encapsulated liposomes exhibited a spherical shape but changed to dumbbell and disk-like shapes after G-actin was polymerized inside the liposomes.[20b] Li and Palmer also studied the effect of actin concentration on the structure of actin-containing liposomes.[20cd] They found that actin-containing liposomes could be extruded through polycarbonate membranes with a pore size of 400 – 600 nm. At low actin concentration (i.e., 0.1 mg/mL), the morphology of these liposomes is spherical in shape. As actin concentration was increased, the morphology changed to a disk-like shape (1 mg/mL) and then back to a spherical shape (5 mg/mL).[20c] These results indicate that the formation of a bundle of actin filaments can affect the morphology of soft lipid bilayers and alter structural strength.

By encapsulating actin into the aqueous core of liposomes, the circulatory half-life was significantly increased from 19 hours for plain liposomes (without actin) to 35 hours for actin-containing liposomes.[20cd] These findings suggest that extended circulatory persistence is desirable for drug delivery applications, since it avoids repeated drug administration. Actin filaments and bundles also can be modified with myosin II to transport liposomes (as "nano-containers" to encapsulate drugs or other molecules of interest) and single cells across an inorganic surface.[21] Biotinylated liposomes or biotinylated *E. coli* cells engineered to express green-fluorescent protein (GFP) were attached to F-actin or actin bundles labeled with rhodamine-phalloidin and biotin-phalloidin via a neutravidin linkage (Fig. 4a). Fig. 4b shows that the actin bundles loaded with liposomes were found to move across the flow cell surface, while the F-actin preparation was able to transport liposomes. Compared to using actin filaments for drug delivery/transport, the use of microtubules as vehicles for drug delivery is more common.

In recent years, intracellular transport studies have indicated the capacity for well-organized bidirectional nanotransport of individual molecules or vesicles, a process that is supported by

MTs preorganized for cargo transport by kinesin and dynein.[22] This can be reconstructed *in vitro* as a bead assay-based system by fixing MTs on a glass substrate and allowing motors to carry cargos toward the direction defined by the polarities of the MTs. Two important technical challenges to realize further organized molecular systems based on a bead assay-based system are controlling the cargo transport direction by defining the polarities of individual MTs and employing both kinesin and dynein to actively and bidirectionally transport cargos for biochemical assays. Fig. 4c shows the bead assay-based system using multiple motors reconstructed in a nanotrack array proposed by Fujimoto *et al.*[23] This system can regulate the direction of molecular transport and the physical interaction of target molecules by using MTs as vehicles. Molecular transport resulting from the movements of kinesin and dynein caused a collision of the GST and GSH sequences, which was revealed by Q-dot colocalization.

Another potential approach for drug delivery is binding tau protein molecules functionally characterized for their effect on MTs kinesin-based transport. The effect of "roadblocks" created by tau protein molecules bound to the MTs could be examined.[24] Htau40 binds to MTs protofilaments, hindering kinesin-coated bead motion (Fig. 4d). The P301L mutation reduces the MT-binding capability of the tau protein, preventing the generation of "roadblocks" and allowing the unhindered movement of kinesin along the MTs. Multiple kinesin molecules access the MTs surface, jointly contributing to the bead movement. Therefore, if a kinesin molecule encountering a "roadblock" (i.e., tau protein) detaches from the microtubules protofilaments, another kinesin may continue the motion (Fig. 4d). As a result, tau protein "roadblocks" produce an effect of "speed bumps" for the kinesin molecules, causing an overall slowing down of the kinesin-coated beads. By combining tau protein and MTs, we suggest that a drug can be delivered to precise positions.

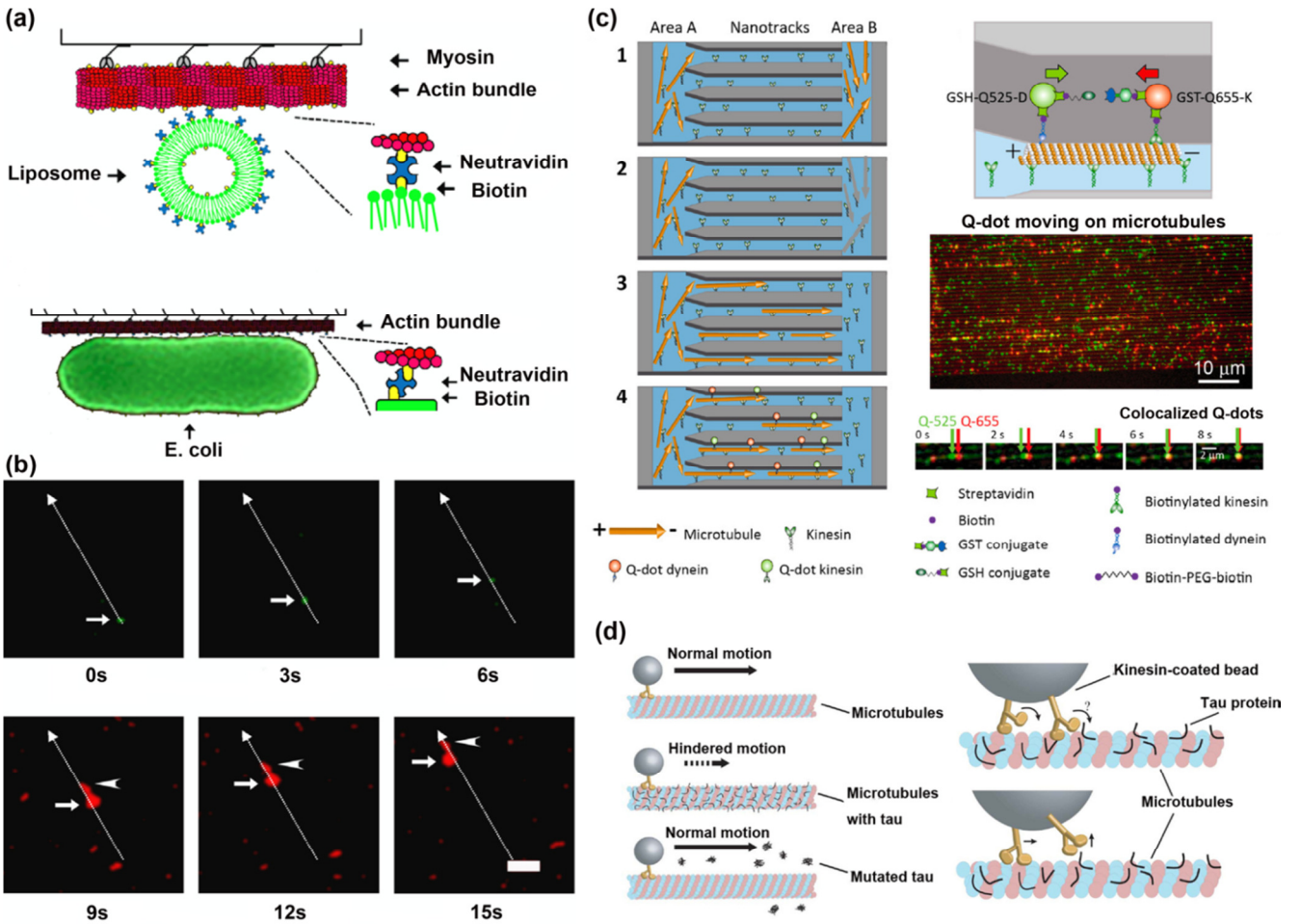

Fig. 4 Potential drug delivery applications using either actin filaments or microtubules. (a) Schematic of biotinylated liposome and *E. coli* cell that have been bound to biotin-labeled actin bundle via a neutravidin linker. (b) Time series images of actin bundle (red; arrowheads) transporting liposome (green; arrows); (a) and (b) are from Ref. 21. (c) The mobility of kinesin and a microtubule dissociation method enable orientation of a microtubule in an array for directed transport of reactive molecules or drugs carried by kinesin or dynein; Ref. 23. (d) Wild type tau (htau40) binds to the MTs creating "roadblocks", and hinders the motion of the beads. The tau protein attached on the microtubule surface may lead to a detachment of the kinesin molecule. The motion may be continued when another kinesin attached to the same bead binds onto the microtubule surface; Ref. 24d.

Nanopatterning

Conventional patterning methods are "top-down" approaches that involve the use of photolithography or electron-beam lithography and subsequent etching and polishing processes. These methods are very useful for constructing two-dimensional (2D) structures with various patterns (e.g., linear patterns, circular patterns, or mixed patterns).[25] Although current nanotechnologies can create patterns as small as several nanometers, expensive equipment and a clean environment are necessary; this limits the applicability for semiconductor industries. In contrast to top-down approaches, molecular self-assembly of peptides and proteins is a "bottom-up" approach that can easily generate 2D or 3D patterns of nanometric size. Actin filaments, one of the cellular fibrous proteins, consist of self-associated monomers of actin. Because actin monomers exhibit guanidine and adenosine triphosphate hydrolytic activity that affords conformational self-assembly, control of actin self-assembly is possible and key to understanding the relationships between protein assembly and a number of diseases.

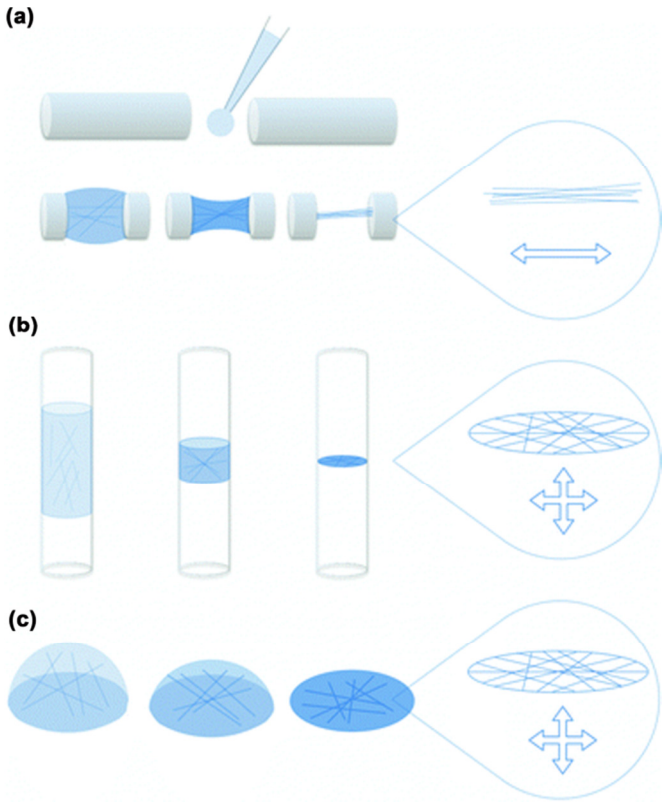

Fig. 5 Methods for aligning fibrous proteins through dehydration. A solution of fibrils was suspended between two sealed capillaries to generate a bundle of fibers (a) or suspended inside a capillary (b) or on a mat or film (c) to generate fibers at the same plane; Ref. 26d.

There are two forms of actin: F-actin is in the form of polymerized fiber, and G-actin is globular in form. Previous studies have shown that G-actin could transform to F-actin when the concentration of salt in solutions increased. Methods for the alignment (patterning) of F-actin have also been widely studied,[26] as shown in Fig. 5. The stretch frame method in Fig. 5a can create a bundle of fibers oriented along the fiber axis (1D alignment), whereas dropping and drying methods in Fig. 5b and 5c can only result in all fibers lying along the same plane. Examining and identifying the orientation of F-actin or other fibrous proteins and peptides was a first step in investigating structural characterization via X-ray diffraction, nuclear magnetic resonance (NMR), and transmission electron microscopy (TEM). Elucidating intramolecular interactions in the aligned (or crystallized) structures would provide structural and mechanistic insights.

Molecular structure holds a key to understanding nature's intricate design mechanisms and blueprints. If we can understand these blueprints and basic materials, perhaps we can begin to mimic the elegance of nature by making beautiful products more cost effectively and with less detrimental environmental consequences. A famous example of leveraging molecular structure characterization is the discovery of DNA structure (amyloid β-peptide) by Fairlie, Craik, and Watson via NMR spectroscopy.[27] Their results may provide new insight to the structural properties of amyloid β-peptides, which are of great relevance to Alzhemier's disease research.

We have attempted to control actin filament organization through biologically-inspired intermediates, allowing us to create a regular nanopattern with a large area.[26e] We first placed individual actin filaments on a pristine glass surface (i.e., a hydrophilic surface) and introduced myosin-II to modify this hydrophilic surface. We then employed the inorganic salt crystallization approach to probe the response of two proteins, actin filament and myosin-II, in order to analyze the resultant spatially localized patterns. Fig. 6a and 6b show fluorescence images of actin filaments on a pristine glass surface and actin filaments on a glass surface treated with myosin-II (non-covalent immobilization), respectively. We quantified the behaviors of both by importing fluorescence images of actin filaments labeled with phalloidin into ImageJ software,[28] and measuring the angle between a single filament and its corresponding horizontal axis to determine the alignment of the filaments on pristine glass, and glass treated with myosin-II. This analysis indicated that the orientation of actin filaments placed on both pristine and functionalized surfaces exhibited orientations of 12º and 38º, respectively. In order to gain further understanding of filament orientation behavior for both samples, we used our previously described salt crystallization method.[26b] Fig. 6c, 6d, and 6e show salt crystallization images of actin filaments on a pristine glass surface, only myosin-II on a glass surface, and actin filaments on a glass surface treated with myosin-II (1 μg/μL), respectively. The orientation of filaments induced by salt crystallization of only actin filaments on a glass surface (Fig. 6c) indicated that salt crystallization induced a more ordered orientation as reflected in the observation of filaments branched in perpendicular directions.

On the other hand, Ionov *et al.* attempted to fabricate stimuli-responsive nanopatterned polymer brushes using MTs as templates.[29] In their study, they used atom transfer radical polymerization to initiate thermoresponsive poly-(N-

isopropylacrylamide) brushes on MTs. Rhodamine-labeled MTs were prepared by self-assembly of α,β-tubulin dimers, and then adsorbed on DDS-coated glass surfaces by perfusing them in buffer solution through a narrow channel between two glass coverslips. The MTs formed chemical links between neighboring amino groups after crosslinking by glutaraldehyde and lysine residues (Fig. 6f). After treating with 2,2′-(ethylenedioxy)bis(ethylamine) and bromo-2-methylpropanoyl bromide, the modified MTs possessed an undeformed rod-like shape (Fig. 6g). The synthesized polymer brushes were modified on MTs by adding fluorescein o-acrylate for the polymerization of N-isopropylacrylamide (Fig. 6h).

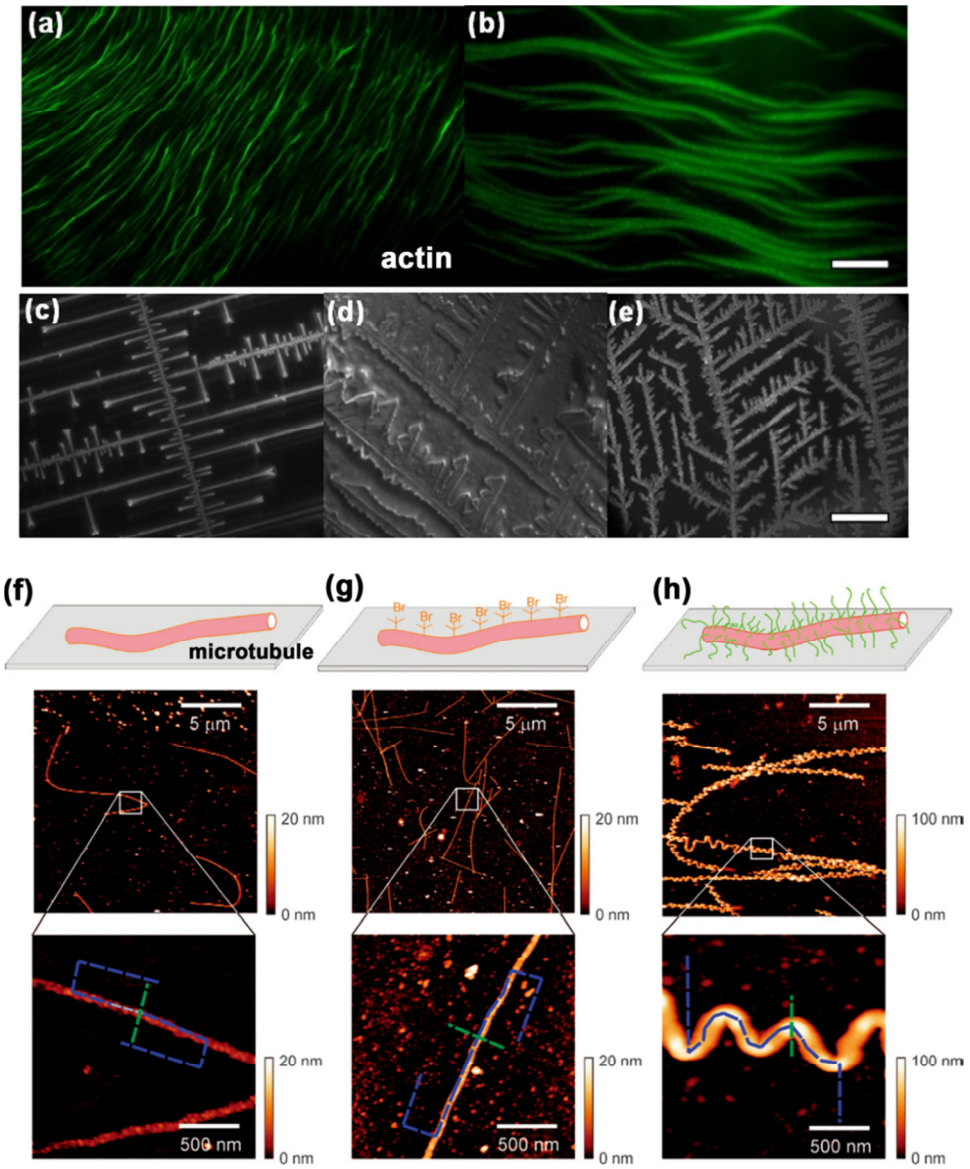

Fig. 6 Actin filament organization on pristine and functionalized glass surfaces. (a) Fluorescence image of actin filaments on a pristine glass surface. (b) Fluorescence image of actin filaments on a glass surface modified with myosin-II. Scale bar = 1 μm. Optical images of the salt crystallization related to the actin filaments presence for (c) only actin filaments on a pristine glass surface, (d) only myosin-II on a glass surface, and (e) actin filaments on a glass surface modified with myosin-II, respectively. Scale bar = 1 μm; Ref. 26e. Morphology of microtubules at different stages of the modification procedure via AFM: (f) after crosslinking with glutaraldehyde, (g) after immobilization of initiator, and (h) after grafting of poly-(N-isopropylacrylamide–fluorescein o-acrylate); Ref. 29.

Recently, macroscale alignment has attracted significant scientific attention. A salting-out strategy has been reported to create macroscale parallel assays of peptide nanotubes.[2a] The addition of anions (e.g., SO_4^{2-}) is efficient for precipitating positively charged peptides, and such salt-induced precipitation is a well-known technology for purification of charged peptides.[30] In contrast, gradual removal of salts would allow one to re-dissolve charged peptides and arrange them in an ordered direction. The driving forces for such macroscopic orientation include hydrophobic/hydrophilic forces and hydrogen bonding. A surface micropatterning method has also been reported to geometrically control the growth and alignment of actin.[31] This study further demonstrates that actin-filament orientation could determine the interactions between

two actin filaments and the formation of actin bundles. Because it is known that the spatial and temporal modulation of the environment exerts great influence on actin cytoskeleton architectures, causing different cell morphologies, a defined geometrical boundary condition could help clarify the effects of spatial arrangements within actin-filament network architectures.

Nanofabrication

Molecular self-assembly has been considered a "bottom-up" approach to efficiently build up nanomaterials. DNA and self-assembled peptides have been widely used as templates for metal deposition. Metal nanowires such as silver,[32] gold,[33] platinum,[34] palladium,[35] and copper[36] have been successfully synthesized using DNA as a template. Cationic metal ions can effectively interact with anionic phosphoric groups of DNA, and subsequent reduction methods including UV irradiation, thermal treatment, or chemical reducing agents can convert metal ions into metal along the DNA template, resulting in metal nanowires of uniform size. Reches and Gazit used self-assembled peptide (i.e., the Alzheimer's-amyloid diphenylalanine structural motif) to form nanotubes.[37] Silver nanowires were then generated inside the peptide nanotubes by impregnation and reduction of silver ions. An enzyme (i.e., proteinase K) was then applied to degrade the diphenylalanine peptides, resulting discrete and enzymatically stable nanowires with a long, persistent length. In this section, we will mainly focus on the use of actin filaments to develop functional nanowires because there is less research regarding the use of MTs.

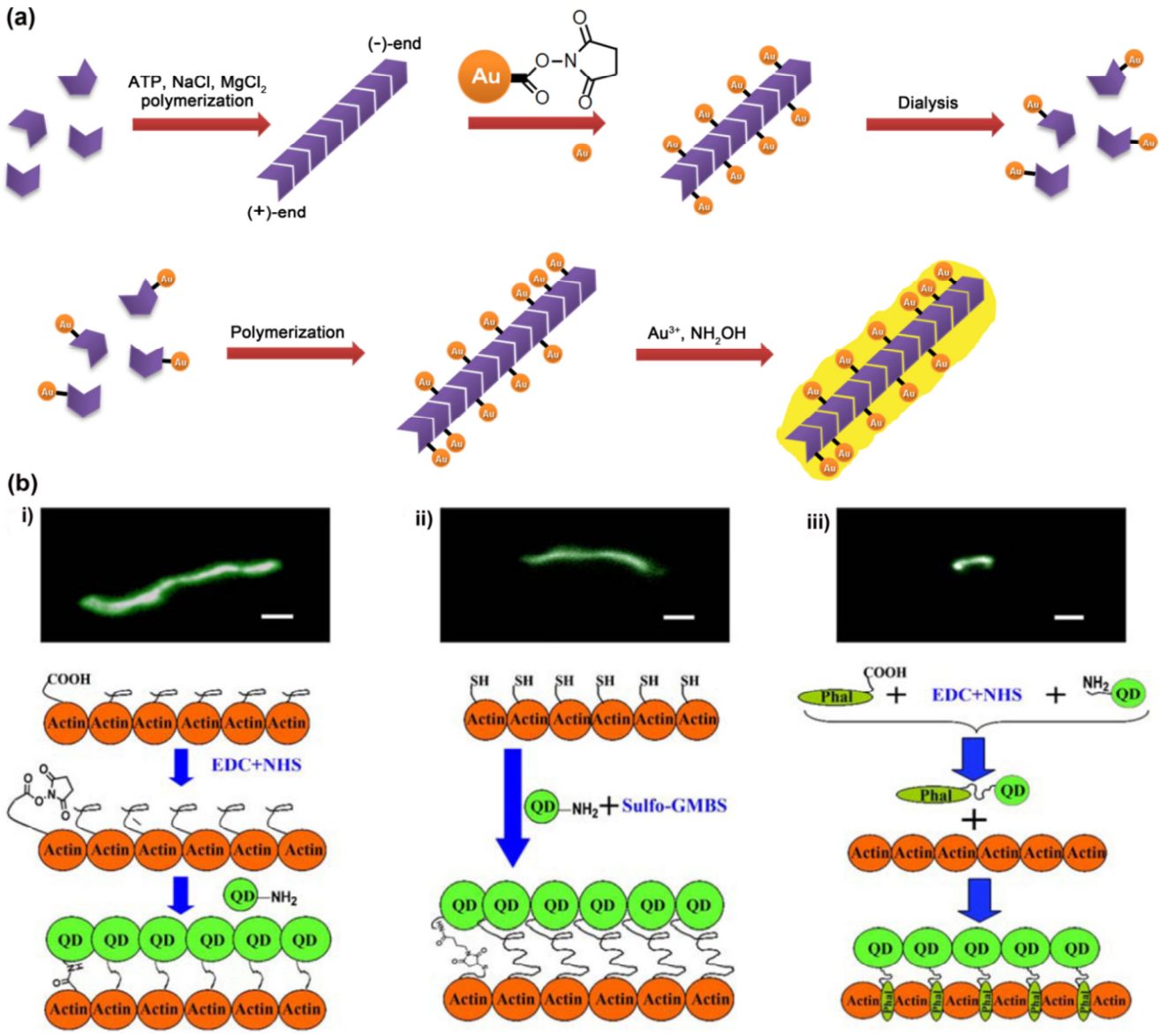

Fig. 7 (a) Scheme for the synthesis of actin-assembled Au nanowires; Ref. 38. (b) Schematic diagrams of three methods of fabrication of QD nanowires using F-actin as a template (bottom) and fluorescence images of QD-actin nanowires; Ref. 39.

G-actin has also been used as a molecular building block for creating metallic nanowires.[38] Although G-actin has a globular structure, it undergoes polymerization when ATP, Mg^{2+}, and K^+ are present. This ATP-driven polymerization converts G-actin monomers to F-actin filaments, which is an important process for cell mobility and cell division. The growth of F-actin filaments can be controlled by thymosin and profilin. The former inhibits the polymerization process by binding to G-actin, while the latter promotes the monomeric addition to the end of F-actin filaments by binding to G-actin. As shown in Fig. 7a,[38] after the formation of F-actin filaments and the addition of gold nanoparticles (Au NPs, 1.4nm) and *N*-hydroxysuccinimide active ester, Au NPs/F-actin composites could be obtained. The removal of ATP, Mg^{2+}, and K^+ degraded the composites into Au NPs/G-actin monomers, as confirmed by AFM and STEM (scanning transmission electron microscope). Interestingly, these Au NPs/G-actin monomers could be re-polymerized into Au NPs/F-actin filaments. Subsequent enlargement of the Au NPs by reduction of gold ions would eventually yield continuous gold nanowires (Au NWs). Au NWs with lengths of 2-3 μm and an average height of 80-100 nm, characteristics controlled by metal deposition time, could be obtained via this self-assembly, F-actin templating process. It is worth noting that, instead of direct coupling of Au NPs to G-actin monomers, coupling of Au NPs to F-actin filaments and subsequent depolymerization of Au NPs/F-actin filament into Au NPs/G-actin monomers are two essential steps for successfully achieving Au NWs. This is because the direct coupling of Au NPs to G-actin monomers blocked the linkage between two Au NPs/G-actin monomers.

The self-assembly, F-actin templating process above could be further expanded to prepare structures such as actin-Au NWs-actin and Au NWs-actin-Au NWs, and these patterned actin-based Au NWs could be used as bio-nanotransporters. When these patterned actin-based Au NWs were placed onto a myosin-coated surface, the nanowires were strongly linked with myosin. After the addition of ATP-Mg^{2+} containing buffer, the linkage between F-actin and myosin could be broken, thus leading to the movement of the patterned actin-based Au NWs.

Yao *et al*. used F-actin as a template for the assembling of water-soluble quantum dots (QDs) into nanowires.[39] The unique electronic and optical properties of QDs, together with advances in QD synthesis and bio-functionalization paved the way for potential QD nanowire applications for electro-optical and biomolecular devices. The cross-linking approaches Yao *et al.* proposed for the fabrication of biomolecule-nanoparticle hybrid systems were described as follows: i) attach amino-QDs to the carboxyl groups of F-actin via NHS-EDC cross-linker; ii) use a bifunctional cross-linker sulfo-GMBS, which contains an amine-reactive sulfo-NHS ester at one end and a thiol-reactive maleimide group at the other end; and iii) QDs were conjugated first with phallacidin by a EDC-NHS-mediated cross-linking reaction and then incubated with F-actin for noncovalent binding (Fig. 7b). In their study, they demonstrated that F-actin can be used as a scaffold for the assembly of one-dimensional QDs arrays or nanowires. Tightly packed on an actin filament, the QDs will be in close enough contact to transport electrons along the filament and emit light.

Metal nanowire fabrication via actin-templating shows great potential as a new nanoscale machine that can be operated by biomolecules. In addition, actin columns in controlled shapes and sizes can be self-assembled and joined to establish connections, and the connections can be metallized with gold nanoparticles, allowing an electrical current to pass between the two surfaces for microelectronics applications.

Conclusions

An overview of recent developments and applications for leveraging cell structures as building block nanomaterials (actin filaments and MTs in this study) has been provided in this article. Actins interact to form braids, bundles, layers, and columns whose architecture and mechanical properties regulate and control cell shape. The capacity to prepare individual actin filaments and subsequently use them for nanopatterning and functional nanowire manufacture has been illustrated here. In regards to MTs, the proposed approach of *in vitro* kinesin-based transport using reconstructed suspended MTs may be a promising method for the detection and characterization of molecular factors regulating intracellular transport and as a vehicle for drug delivery. These results demonstrate that the self-assembly process of actin filaments may have unanticipated industrial applications. In the near future, we look forward to continued improvements in these fields as ideas are shared and applications are made across disciplines.

Acknowledgements

We would like to thank the National Science Council of Taiwan for financially supporting this research under Contract No. NSC 101-2628-E-007-011-MY3, NSC 102-2221-E-007-031 (to C.-M. Cheng), and 101-2628-E-002-015-MY3 (to K. C.-W. Wu). National Health Research Institute (NHRI) of Taiwan (ME-102-PP-14; to K. C.-W. Wu), National Taiwan University (102R7842 and 102R7740; to K. C.-W. Wu) and Center of Strategic Materials Alliance for Research and Technology (SMART Center), National Taiwan University (102R104100; to K. C.-W. Wu).

Notes and references

[a] Department of Chemical Engineering, National Taiwan University, Taipei 10617, Taiwan.
[b] Institute of Nanoengineering and Microsystems, National Tsing Hua University, Hsinchu 30013, Taiwan. E-mail: chaomin@mx.nthu.edu.tw
†These authors contributed equally.

1 (*a*) E. Katz and I. Willner, *Angew. Chem., Int. Ed.*, 2004, **43**, 6042; (*b*) C. M. Niemeyer, *Angew. Chem., Int. Ed.*, 2001, **40**, 4128; (*c*) H. Gu, K. Xu, C. Xu and B. Xu, *Chem. Commun.*, 2006, **9**, 941; (*d*) R. Baron, B. Willner and I. Willner, *Chem. Commun.*, 2007, **10**, 323; (*e*) I. Willner, B. Basnar and B. Willner, *FEBS J.*, 2007, **274**, 302; (*f*) N. C. Seeman, *Annu. Rev. Biochem.*, 2010, **79**, 65.

2 (*a*) M. F. Krendel and E. M. Bonder, *Cell Motil. Cytoskeleton*, 1999, **43**, 296; (*b*) T. D. Pollard, L. Blanchoin and R. D. Mullins, *Annu. Rev. Biophys. Biomol. Struct.*, 2000, **29**, 545; (*c*) R. Heald and E. Nogales, *J. Cell Sci.*, 2002, **115**, 3; (*d*) C. I. Lacayo, Z. Pincus, M. M. VanDuijn, C. A. Wilson, D. A. Fletcher, F. B. Gertler, A. Moqilner and J. A. Theriot, *PLoS Biol.*, 2007, **5**, e233; (*e*) D. Nanba, F. Toki, N. Matsushita, S. Matsushita, S. Higashiyama and Y. Barrandon, *EMBO Mol. Med.*, 2013, **5**, 640.

3 (*a*) K. C. Holmes, *Nature*, 2009, **457**, 389; (*b*) T. Oda, M. Iwasa, T. Aihara, Y. Maéda and A. Narita, *Nature*, 2009, **457**, 441.

4 (*a*) P. Matsudaira, J. Bordas and M. H. Koch, *Proc. Natl. Acad. Sci. USA*, 1987, **84**, 3151; (*b*) O. Pelletier, E. Pokidysheva, L. S. Hirst, N. Bouxsein, Y. Li and C. R. Safinya, *Phys. Rev. Lett.*, 2003, **92**, 148102.

5 (*a*) J. D. Kakisis, C. D. Liapis and B. E. Sumpio, *Endothelium*, 2004, **11**, 17; (*b*) J. J. Wille, C. M. Ambrosi and F. C.-P. Yin, *J. Biomech. Eng.*, 2004, **126**, 545; (*c*) R. Kaunas, P. Nguyen, S. Usami and S. Chien, *Proc. Natl. Acad. Sci. USA*, 2005, **102**, 15895.

6 H.-J. Hsu, C.-F. Lee and R. Kaunas, *PLoS ONE*, 2009, **4**, e4853.

7 J. Liao, L. Yang, J. Grashow and M. S. Sacks, *Acta Biomater.*, 2005, **1**, 45.

8 J. H.-C. Wang, P. Goldschmidt-Clermont, J. Wille and F. C.-P. Yin, *J. Biomech.*, 2001, **34**, 1563.

9 (*a*) M. Haqa, A. Chen, D. Gortler, A. Dardik and B. E. Sumpio, *Endothelium*, 2003, **10**, 149; (*b*) T. Lee and B. E. Sumpio, *Biotechnol. Appl. Biochem.*, 2004, **39**, 129; (*c*) K. Nishimura, W. Li, Y. Hoshino, T. Kadohama, H. Asada, S. Ohgi and B. E. Sumpio, *Am. J. Physiol.-Cell Ph.*, 2005, **290**, C812.

10 C.-M. Cheng and P. R. LeDuc, *Adv. Mater.*, 2008, **20**, 953.

11 J. E. Smith, *Vet. Pathol.*, 1987, **24**, 471.

12 J. Li, A. Shariff, M. Wiking, E. Lundberg, G. K. Rohde and R. F. Murphy, *PLoS ONE*, 2012, **7**, e50292.

13 J. Howard, A. Hudspeth and R. Vale, *Nature*, 1989, **342**, 154.

14 (*a*) C. Z. Dinu, D. B. Chrisey, S. Diez and J. Howard, *Anat. Rec.* (Hoboken), 2007, **290**, 1203; (*b*) C. Z. Dinu, J. Opitz, W. Pompe, J. Howard, M. Mertig and S. Diez, *Small*, 2006, **2**, 1090; (*c*) H. Hess, J. Clemmens, C. Brunner, R. Doot, S. Luna, K. H. Ernst and V. Vogel, *Nano Lett.*, 2005, **5**, 629; (*d*) H. Hess and V. Vogel, *J. Biotechnol.*, 2001, **82**, 67.

15 (a) T. Kouyama and K. Mihashi, Eur. *J. Biochem.*, 1980, **105**, 279; (b) J. A. Cooper, S. B. Walker and T. D. Pollard, *J. Muscle Res. Cell Motil.*, 1983, **4**, 253; (c) N. Suzuki, H. Miyata, S. Ishiwata and K. Kinosita Jr., *Biophys. J.*, 1996, **70**, 401; (d) D. A. Schafer, P. B. Jennings and J. A. Cooper, *J. Cell Biol.*, 1996, **135**, 165.

16 ATP-buffer is general actin buffer, from *Cytoskeleton*; No.: BSA01. This buffer contains 5 mM Tris-HCl (pH 8.0) and 0.2 mM $CaCl_2$.

17 This is a 10 X solution that contains 500 mM KCl, 20 mM $MgCl_2$ and 10 mM ATP.

18 (*a*) M. L. Shelanski, F. Gaskin and C. R. Cantor, *Proc. Natl. Acad. Sci. U.S.A.*, 1973, **70**, 765; (*b*) R. C. Jr. Williams and J. C. Lee, *Methods Enzymol.*, 1982, **85**, 376; (*c*) R. B. Vallee, *Methods Enzymol.*, 1986, **134**, 89; (*d*) J. Avila, H. Soares, M. L. Fanarraga and J. C. Zabala, *Curr. Protoc. Cell Biol.*, 2008, **39**, 3.29.1.

19 (*a*) K. Rajagopal and J. P. Schneider, *Curr. Opin. Struct. Biol.*, 2004, **14**, 480; (*b*) K. Morris and L. Serpell, *Chem. Soc. Rev.*, 2010, **39**, 3445.

20 (*a*) J. D. Cortese, B. Schwab, C. Frieden and E. L. Elson, *Proc. Natl. Acad. Sci. USA*, 1989, **86**, 5773; (*b*) H. Miyata and H. Hotani, *Proc. Natl. Acad. Sci. USA*, 1992, **89**, 11547; (*c*) S. Li and A. F. Palmer, *Langmuir*, 2004, **20**, 4629; (*d*) S. Li and A. F. Palmer, *Langmuir*, 2004, **20**, 7917.

21 H. Takatsuki, H. Tanaka, K. M. Rice, M. B. Kolli, S. K. Nalabotu, K. Kohama, P. Famouri and E. R. Blough, *Nanotechnology*, 2001, **22**, 245101.

22 (*a*) N. Hirokawa, *Science*, 1998, **279**, 519; (*b*) B. Alberts, A. Johnson, J. Lewis, M. Raff, K. Roberts and P. Walter, *Molecular Biology of the Cell, 4th ed.*, New York, 2002, 1616.

23 K. Fujimoto, M. Kitamura, M. Yokokawa, I. Kanno, H. Kotera and R. Yokokawa, *ACS Nano*, 2013, **7**, 447.

24 (*a*) T. Korten and S. Diez, *Lab Chip*, 2008, **8**, 1441; (*b*) S. Taira, Y.-Z. Du, Y. Hiratsuka, K. Konishi, T. Kubo, T. Q. P. Uyeda, N. Yumoto and M. Kodaka, *Biotechnol. Bioeng.*, 2006, **95**, 533; (*c*) M. Bachand, A. M. Trent, B. C. Bunker and G. D. Bachand, *J. Nanosci. Nanotechnol.*, 2005, **5**, 718; (*d*) M. C. Tarhan, Y. Orazov, R. Yokokawa, S. L. Karsten and H. Fujita, *Lab Chip*, 2013, **13**, 3217.

25 (*a*) C.-W. Wu, T. Aoki and M. Kuwabara, *Nanotechnology*, 2004, **15**, 1886; (*b*) C. W. Wu, T. Ohsuna, T. Edura and K. Kuroda, *Angew. Chem. Int. Ed. Engl.*, 2007, **46**, 5364.

26 (*a*) D. Popp, V. V. Lednev and W. Jahn, *J. Mol. Biol.*, 1987, **197**, 679; (*b*) C.-M. Cheng and P. R. LeDuc, *J. Am. Chem. Soc.*, 2007, **129**, 9546; (*c*) C.-M. Cheng and P. R. LeDuc, *Appl. Phys. Lett.*, 2008, **93**, 174106; (*d*) K. Morris and L. Serpell, *Chem. Soc. Rev.*, 2010, **39**, 3445; (*e*) M. Hazar, R. L. Steward Jr., C.-J. Chang, C. J. Orndoff, Y. Zeng, M.-S. Ho, P. R. LeDuc and C.-M. Cheng, *Appl. Phys. Lett.*, 2011, **99**, 233701.

27 M. Coles, W. Bicknell, A. A. Watson, D. P. Fairlie and D. J. Craik, *Biochemistry*, 1998, **37**, 11064.

28 downloaded from the National Institutes of Health; http://rsb.info.nih.gov/ij/download.html

29 L. Ionov, V. Bocharova and S. Diez, *Soft Matter*, 2009, **5**, 67.

30 Y. K. Kryschenko, S. R. Seidel, A. M. Arif and P. J. Stang, *J. Am. Chem. Soc.*, 2003, **125**, 5193.

31 A. C. Reymann, J. L. Martiel, T. Cambier, L. Blanchoin, R. Boujemaa-Paterski and M. Thery, *Nat. Mater.*, 2010, **9**, 827.

32 (*a*) E. Braun, Y. Eichen, U. Sivan and G. Ben-Yoseph, *Nature*, 1998, **391**, 775; (*b*) S. Cui, Y. Liu, Z. Yang and X. Wei, *Mater. Des.*, 2007, **28**, 722; (*c*) S. H. Han and J. S. Lee, *Langmuir*, 2012, **28**, 828.

33 (*a*) F. Patolsky, Y. Weizmann, O. Lioubashevski and I. Willner, *Angew. Chem. Int. Ed.*, 2002, **41**, 2323. (*b*) A. N. Sokolov, F. L. Yap, N. Liu, K. Kim, L. Ci, O. B. Johnson, H. Wang, M. Vosgueritchian, A. L. Koh, J. Chen, J. Park and Z. Bao, *Nat. Commun.*, 2013, **4**, 2402.

34 J. Richter, M. Mertig, W. Pompe, I. Monch and H. K. Schackert, *Appl. Phys. Lett.*, 2001, **78**, 536.

35 M. Mertig, L. C. Ciacchi, R. Seidel, W. Pompe and A. De Vita, *Nano Lett.*, 2002, **2**, 841.

36 C. F. Monson and A. T. Woolley, *Nano Lett.*, 2003, **3**, 359.

37 M. Reches and E. Gazit, *Science*, 2003, **300**, 625.

38 F. Patolsky, Y. Weizmann and I. Willner, *Nat Mater*, 2004, **3**, 692.

39 L. Yao, G. O. Andreev, Y. K. Reshetnyak and O. A. Andreev, *Anal. Bioanal. Chem.*, 2009, **395**, 1563.

